REPORT DOCUMENTATION PAGE

Form Approved
OMB No. 0704-0188

1. AGENCY USE ONLY (Leave blank)	2. REPORT DATE	3. REPORT TYPE AND DATES COVERED
	1995	Interim

4. TITLE AND SUBTITLE
Electronic Structure of Donor-spacer-Acceptor Molecules of Potential Interest for Molecular Electronics IV: Geometry and Device Properties of P3CNQ and Q3CNQ

5. FUNDING NUMBERS
N00014-90-J-1608
G

6. AUTHOR(S)
Anders Broo and Michael C. Zerner

7. PERFORMING ORGANIZATION NAME(S) AND ADDRESS(ES)
University of Florida
Department of Chemistry
Gainesville, FL 32611 USA

8. PERFORMING ORGANIZATION REPORT NUMBER

9. SPONSORING/MONITORING AGENCY NAME(S) AND ADDRESS(ES)
Office of Naval Research
Chemistry Division Code 1113
Arlington, VA 22217-5000

10. SPONSORING/MONITORING AGENCY REPORT NUMBER
Technical Report 28

11. SUPPLEMENTARY NOTES
Molecular Physics, In Press

12a. DISTRIBUTION/AVAILABILITY STATEMENT
This document has been approved for public release: its distribution is unlimited.

12b. DISTRIBUTION CODE

13. ABSTRACT (Maximum 200 words)

See attached Abstract.

19950427 011

14. SUBJECT TERMS	15. NUMBER OF PAGES 28
	16. PRICE CODE

17. SECURITY CLASSIFICATION OF REPORT	18. SECURITY CLASSIFICATION OF THIS PAGE	19. SECURITY CLASSIFICATION OF ABSTRACT	20. LIMITATION OF ABSTRACT
Unclassified	Unclassified	Unclassified	SAR

OFFICE OF NAVAL RESEARCH

GRANT or CONTRACT N00014-90-J-1608

R&T CODE 4131057- - - 01

Technical Report No. 28

Electronic Structure of Donor-spacer-Acceptor Molecules of Potential Interest for Molecular Electronics IV: Geometry and Device Properties P3CNQ and Q3CNQ

by

Anders Broo and Michael C. Zerner

Prepared for Publication or Published

in

Molecular Physics

University of Florida
Department of Chemistry
Quantum Theory Project
Gainesville, FL 32611-8435

April 18, 1995

Electronic Structure of Donor-spacer-Acceptor Molecules of Potential Interest for Molecular Electronics IV: Geometry and Device Properties of P3CNQ and Q3CNQ.

by

Anders Broo[a] and Michael C. Zerner

Quantum Theory Project

University of Florida

Gainesville, Florida 32611-8435

Z-β-(1-hexadecyl-4-quinolinium)-α-cyano-4-styryldicyanomethanide ($C_{16}H_{33}$-Q3CNQ) and the pyridinium analogue Z-β-(1-hexadecyl-4-pyridinium)-α-cyano-4-styryldicyanomethanide ($C_{16}H_{33}$-P3CNQ) are two very promising candidates for molecular device design. We obtain the geometry of the ground and excited state of these systems using the PM3 quantum mechanical model. The absorption spectra in vacuum and in solution are calculated using the INDO/CI model, and compared to experimental spectra. The solvatochromic shift of the absorption spectra was calculated using a self-consistent reaction field approach. The observed bleaching of Langmuir-Blodgett films and solutions of $C_{16}H_{33}$-Q3CNQ and $C_{16}H_{33}$-P3CNQ is explained as resulting from a twisted configuration formed without barrier upon absorption into a twisted intramolecular charge transfer state. The observed rectification is explained from a ground state potential energy surface with two minima, one of which is characterized by a very large dipole moment. The relative energy of these minima is easily shifted by an electric field. The overall electron transport rate is found to be very small due to the small electronic coupling between the mono-layers of the L-B film. Thus, the electron transport through the sample is likely through defects of the L-B film. A way to increase the electronic coupling between the mono-layers is also discussed.

---

a) Permanent address Department of Physical Chemistry, Chalmers University of Technology 412 96 Göteborg, Sweden.

1. Introduction.

In a previous series of papers the electron structure of organic molecules of the type electron Donor-bridge-Acceptor (D-b-A) that are of potential interest for molecular electronics have been investigated [1]. In the last paper in this series the geometry and electron structure of Z-β-(1-methyl-2-pyridinium)-α-cyano-4-styryldicyanomethanid (α-P3CNQ) were calculated using several different quantum chemical methods and compared with experimental information [1c]. One of the conclusions from that work was that a single determinant description (restricted Hartree-Fock) of the ground state was not sufficient to describe the geometry with acceptable accuracy, a result that we found to be independent of the model Hamiltonian used. (Two semi-empirical Hamiltonians, AM1 and PM3, and *ab initio* methods, with different basis sets, were used in that work.) The best agreement between the calculated geometry and the experimental geometry was obtained with the PM3 model using a four determinant description (4x4CI/PM3). The PM3 model has thus been used for most of the geometry determinations in this paper. To check the accuracy of the PM3 calculations, several *ab initio* geometry optimizations have also been performed to calibrate the semi-empirical calculations.

The photochromic and non-linear optical properties of Z-β-(1-hexadecyl-4-quinolinium)-α-cyano-4-styryl-dicyanomethanide ($C_{16}H_{33}$-Q3CNQ) and Z-β-(1-hexadecyl-4-pyredenium)-α-cyano-4-styryl-dicyanomethanide ($C_{16}H_{33}$-P3CNQ) Langmuir-Blodgett (L-B) films has been experimentally investigated by Ashwell et al. [2]. The chemical structure of these two molecules is depicted in figure 1.

* Fig. 1 *

Ashwell et al. [2] showed that if a L-B film was irradiated with light overlapping the "charge transfer band" of the absorption spectrum the films of both $C_{16}H_{33}$-Q3CNQ and $C_{16}H_{33}$-P3CNQ loose their blue-green color and become transparent. If the molecules are dissolved in a solvent the bleaching effect disappears after some minutes. A preliminary theoretical investigation of this phenomenon was

presented in 1993 by Broo [3]. This phenomenon will be investigated by means of quantum chemical calculations in this paper.

Another series of very interesting experiments, performed by Ashwell and co. workers although still controversial, will also be discussed here [4]. In these experiments mono-layers or multi-layers of L-B film consistent of $C_{16}H_{33}$-Q3CNQ were transferred to a platinum [4a] or silver [4b] surface. The polar group (Q3CNQ) is oriented towards the nobel metal surface (Z type LB film). In the multi-layer films the next layer is oriented in the same way so that the polar end is in close contact with the non-polar tail of the former layer. A second metal layer (magnesium) was then applied on top of the L-B film. A voltage was applied over the metal/L-B film/ metal junction. The voltage signal was swept in both forward and backward direction and the current flow was recorded. The current response was found to be asymmetric with respect to the polarity of the applied electric field. The asymmetric current response (I-V characteristic) was interpret as molecular rectification. An alternative explanation of the phenomenon in which the interaction between the electrodes and molecular head group produced a rectifying interfacial region was discussed in the original study [4a] and by Metzger et al. [5] and Bloor [6]. Somewhat later, however, Ashwell et al. [4b] demonstrated that the rectification is indeed taking place in the L-B film by an experiment in which 22 layers of ω-tricosenoic acid L-B film were applied on both metal surfaces before the L-B film of $C_{16}H_{33}$-Q3CNQ was applied. The ω-tricosenoic acid L-B film diminishes the interaction between the metal surfaces and the $C_{16}H_{33}$-Q3CNQ L-B film. The experiment with a passive LB film close to the electrode surfaces prevents the formation of Schottky barriers, but there might still be problems with short-circuits since the resistivity of the metal/L-B film/metal junction were not measured. When the electric field is applied in one direction (forward bias) the L-B film acts as a conductor. When the electric field is reversed (negative bias) the L-B film acts as an insulator. In this work we will investigate this phenomenon and suggest a mechanism for the switching phenomenon. Molecular rectification was originally put forward by Aviram and Ratner [7]. In that work Aviram and Ratner suggested that oriented films of the bicyclo[2,2,2]octane bridged donor acceptor molecule, TTF-σ-TCNQ would show rectifying character. The work of Aviram and Ratner was based on theoretical calculations and electron transfer theory in the solid state. In this work we will use the Marcus and Hush [8] model for electron transfer to describe the rectifying character of the L-B film in an electric field.

2. Calculational Methods.

2.1 Geometry optimization.

The geometry optimizations were performed with the MOPAC 6.0 program package [9] using the PM3 Hamiltonian. Some reference geometry optimizations at the *ab initio* level were also performed for $C_{16}H_{33}$-Q3CNQ to investigate the nature of the ground state. The *ab initio* calculations were performed with the GAMESS program [10]. Two standard basis sets were used; the minimal basis set STO-3G (HF/STO-3G) and the split valence 3-21G (HF/3-21G) basis set. Based on our previous experiences [1c] the ground state of the molecules was optimized using a four determinant description (4x4CI/PM3). The first singlet root of the CI calculation represents the ground state. The geometries of the first excited state of $C_{16}H_{33}$-Q3CNQ and $C_{16}H_{33}$-P3CNQ were obtained by selecting the second singlet root of a four determinant CI calculation and optimizing the geometry for that root. In order to reduce the size of the problem we assumed that the hydrophobic tail of the two molecules could be represented by a CH_3 group, C20 in figures 4 and 5. The eventual geometry changes of the "active" part of the molecule introduced by cutting of the hydrophobic tail is assumed to be small. The abbreviations P3CNQ and Q3CNQ will hereafter be used when the hydrophobic tail is replaced with a CH_3 group. The same convergence criterion as that used in reference 1c was used in this work.

2.2. Absorption spectra.

The absorption spectra were calculated with the INDO/S Hamiltonian using the ZINDO program package [11]. The spectra were calculated from configuration interaction calculations that includes single excitations only (CIS). The active CI space was selected to include all $\pi \rightarrow \pi^*$ and $n \rightarrow \pi^*$ transitions. Solvent influence on the calculated spectra is accounted for via the self-consistent reaction field (SCRF) method [12].

3. Electron Transfer Theory.

Marcus and Hush [8] have developed a theory for electron transfer (ET) reactions based on classical activated-complex theories and a semi-classical treatment of the barrier penetration. Later several extensions were made to include quantum mechanical corrections and non-classical barrier penetration [13]. All of these theories rely on the Born-Oppenheimer approximation that separate the nuclear motions from electronic motion, generating potential energy surfaces for nuclear positions. In analogy with the theory for electronic spectroscopy the actual electron "jump" is assumed to be very fast and the nuclear configuration will not change during the electron transfer (Franck-Condon principle). A schematic picture of an electron transfer reaction is found in figure 2.

* Fig 2. *

In the original ET theory by Marcus and Hush the intra-molecular or bridged ET rate is given by

$$k_{et} = \nu_n \exp(-\Delta G^*/RT), \qquad (1)$$

where ΔG^* is the free energy required to produce the activated complex, see figure 2, and ν_n is an average frequency with which the activated complex is formed. In a semi-classical treatment of the barrier penetration the probability that the system reaching the activated complex configuration will end up in the product state is less than unity. That regime is called non-adiabatic electron transfer in contrast to the situation described by equation 1 where the electron transfer is said to be adiabatic. In the non-adiabatic regime the electron transfer rate in equation 1 must be multiplied by an electronic factor κ_{el}, which is less or equal to one. The electronic factor is given by

$$\kappa_{el}=\pi^2\Delta^2/(2h\nu_n(\pi RT\lambda)^{1/2}), \qquad (2)$$

where Δ is the electronic coupling between the reactants and the products at the avoided crossing (figure 2), h is the Plank constant and λ is the total reorganization energy of all parts of the system upon electron transfer. The reorganization energy may be divided in two parts

$$\lambda = \lambda_{in} + \lambda_{out}, \tag{3}$$

where λ_{in} can be expressed in terms of the changes in the molecular bond lengths between the reactant and product configuration and λ_{out} is associated with the rearrangement of the surrounding media when an electron is transferred. The free energy of activation ΔG^0 can be written in terms of the free energy of the reaction and the total molecular reorganization energy if the potential energy of the reactant and product configurations can be described by two harmonic potentials with the same Hook's constant:

$$\Delta G^* = \lambda/4 \ (1+\Delta G^0/\lambda)^2. \tag{4}$$

The final equation for the ET rate is then given by

$$k_{et} = (\pi^2\Delta^2/(2h(\pi RT\lambda)^{1/2})) \exp(-\lambda(1+\Delta G^0/\lambda)^2/4RT). \tag{5}$$

The rate determining factors for bridged ET are thus the free energy of the reaction ΔG^0, the reorganization energy λ and the electronic coupling Δ. The greatest ET rate is obtained when the exponent in equation 5 is zero, i.e. when $-\Delta G^0 = \lambda$. The latter requirement means that the activation barrier vanishes and the double well representation of the ground state in figure 2 collapses into a single well. If now Δ is sufficient large the system becomes a conductor. To achieve metal conduction Δ must be larger than $\lambda/2$ [14]. When the coupling is large enough to support electrical conduction the electron transfer rate is given by equation 1, that situation corresponds to adiabatic electron transfer. Thus, further increase of the electronic coupling will not enhance the electron transport through the molecule.

If we want to describe a molecular rectifier, using the ET theory outlined above, we need to describe the molecule by potential energy surfaces similar to those of figure 2. In figure 3 a hypothetical sequence of potential energy surfaces for a molecular rectifier under negative bias, no bias and forward

bias are presented. Figure 3 is constructed by solving the two interacting state problem by solving the secular determinant in equation 6.

$$\begin{vmatrix} (H_{11} - E) & \Delta / 2 \\ \Delta / 2 & (H_{22} - E) \end{vmatrix} = 0 \qquad (6)$$

If we now assume that H_{11} and H_{22} is given by two harmonic potentials and the bias just shifts H_{22} up or down depending on polarity we get figure 3. The figure is constructed by assuming the electronic coupling is large. If Δ becomes even larger and the two minimum of the potential energy curves are located close to each other along the reaction coordinate (x-axis) the lower double well curve will collapse into a single well with the minimum centered at the crossing point of the diabatic curves (two non-interacting states). An example of the collapse of the double well in to a single well is the so called Creuz-Taube ion ($Ru(NH_3)_5$-pyrazine-$Ru(NH_3)_5^{5+}$) where the odd electron is completely delocalized and by changing the ligands to 2,2'-bipyridine the electron is localized to one of the ruthenium sites [15a]. This competition between localization and delocalization in mixed valence compounds have been studied and classified by Robin and Day [15b]

* Fig. 3*

The requirements of an efficient molecular rectifier are that the applied electric field that is necessary to reach the conducting state must be as small as possible and that the electronic coupling is large. The question then is "how can we achieve these circumstances?" In the next section we discuss this point and investigate how geometry affects the localization/delocalization of the two molecules of interest in this investigation.

4. Results and discussion.

4.1 The ground state and first excited state geometries of P3CNQ and Q3CNQ.

First we want to compare the geometry of P3CNQ, as predicted with the 4x4CI/PM3 method, with the predicted geometry α-P3CNQ [1c]. α-P3CNQ is an analogue molecule to P3CNQ with the CH_3 group bonded to a nitrogen at the position in the pyridine ring. In figure 4 the 4x4CI/PM3 predicted geometry of the ground state and first excited state are depicted.

* Fig. 4 *

The predicted geometry of P3CNQ is very similar to the predicted geometry of α-P3CNQ. The major difference is found in the donor part of the molecule, which is not surprising since the donor parts differ in the two molecules. The predicted geometry of the bridge and donor parts of P3CNQ clearly suggest the ground state to be zwitterionic, due to the double bond character of the C1-C2 bond, see figures 1a and 4. However, the acceptor has some character of the "neutral" resonance structure suggested by somewhat short C4-C7 and C9-C10 bonds, as does the donor with short C17-C18 and C21-C22 bonds. The same bond pattern was also found for α-P3CNQ. We have previously concluded by inspection of the geometry and Mulliken charges of α-P3CNQ that all three possible zwitterionic resonance structures contributed to the ground state of α-P3CNQ [1c]. The geometry and the Mulliken charges from the 4x4CI/PM3 calculation suggest that only one zwitterionic resonance structure contributes to the ground state of P3CNQ. We predict a somewhat smaller torsion angle between the donor plane and the bridge-acceptor plane than that which was found for α-P3CNQ.

The calculations predict a large geometry change upon excitation of P3CNQ. The most striking change is the rotation of the donor part. The donor plane is almost perpendicular to the bridge-acceptor plane in the excited state. Furthermore, all ring carbon-carbon bonds in the donor are now of almost equal length in the excited state. The "neutral" resonance structure character has increased for the acceptor and the C1-C2 bond in the bridge is somewhat shorter in the excited state than that found for the ground state. The dipole moment change upon excitation is very large ($\mu_{g.s.}$=14.7 Debye and $\mu_{e.s.}$=45.5 Debye). The geometry change and dipole moment change upon excitation indicate that the excited state is of twisted intermolecular charge transfer (TICT) type [16]. The first molecular TICT state was found for p-N,N-dimethylaminobenzonirtile (DMABN) [16a]. During the 30 years since

TICT states were first recognized a large number of molecules that forms TICT states have been identified [16]. Most of these molecules have a dual fluorescence spectrum in which two peaks originate from two different excited state geometries. The relative intensity and position of these two fluorescence bands are very solvent dependent. The intensity of the low energy band, which originates from the twisted geometry, is usually favored in polar solvents. The twisted excited state is stabilized by the interaction between the molecular charge distribution and the polar solvent. In this case the twisting of the excited state of P3CNQ is predicted to occur even without the extra stabilization of the solvent. The eigenvectors from the 4x4CI calculations were analyzed at the two optimized geometries and are summarized in table 1. The (non-twisted) ground state description is dominated by the closed-shell configuration, while the description of the non-twisted excited state is mostly a single open-shell singlet configuration. At the twisted geometry the ground state is dominated by the open-shell configuration and the excited state is mostly the closed-shell configuration. Excitation leads to twisting of the molecule. During the twisting the character of the two states changes and at the twisted geometry the ground state now has biradical character and the excited state gains zwitterionic character. This suggests that the twisted geometry corresponds to a local energy minimum on the ground state potential energy surface and a state crossing must have occurred. The two potential energy surfaces look very much like the simple double well potential energy surface in figure 2. This will be further discussed in the next section.

The predicted geometries of the ground state and the first excited state of Q3CNQ is found in figure 5.

* Fig. 5 *

The predicted geometry of the bridge and the donor part of Q3CNQ suggest a zwitterionic ground state and the geometry of the acceptor suggests a "neutral" ground state, similar to the predicted geometries of P3CNQ and α-P3CNQ. An examination of the geometry and dipole moment change upon excitation to the first excited state suggests the same type of TICT state as was found for P3CNQ.

The *ab initio* geometry optimization of Q3CNQ at the HF/STO-3G and HF/3-21G level give similar geometries to that obtained in the HF/PM3 calculation, as we also found to be true for our calculations on α-P3CNQ [1c].

4.2 The absorption spectra and optical memory properties of P3CNQ and Q3CNQ.

P3CNQ in acetonitrile is observed to have an intense band at 15500 cm^{-1} that is ascribed to a charge transfer transition [2a]. At about 30400 cm^{-1} a second band is observed with about half the intensity of the charge transfer band. The absorption spectrum of Q3CNQ is similar, and has a charge transfer band at 14000 cm^{-1} and a second band, split into two overlapping bands, with maxima at about 26500 cm^{-1} and 28700 cm^{-1}. When solutions of either P3CNQ or Q3CNQ are irradiated with light having energies that overlap the charge transfer band, the color of the previously green or green-blue solution disappears. Ashwell [2a] suggested that the bleaching was caused by geometry changes corresponding to a switch from the zwitterionic geometry to the "neutral" geometry. The solution slowly regains the color after some minutes. The predicted absorption spectra of P3CNQ and Q3CNQ are summarized in Table 2. In the spectral calculations the 4x4CI/PM3 geometries are used and the solvent effects are accounted for by the B1-SCRF method [1c]. The solute cavity radius, a_0=6.6 Å, is the same as used in our previous work [1c]. As we demonstrated in the previous section the first excited state of both molecules will relax to a TICT state. To verify this picture we performed multi-reference CI calculations, with the INDO/S Hamiltonian, of the two first singlet states and the lowest triplet state. At the ground state geometry we find the singlet to be most stabile. The first triplet state is found at about 4700 cm^{-1} above the ground state and the first singlet excited state is found at about 16000 cm^{-1}. Using the excited state geometry we predicted the triplet state and the lowest singlet state at almost the same energy; the triplet was found to be more stabile by 19 cm^{-1}. The lowest singlet state is dominated by an open-shell configuration (a single excitation from HOMO to LUMO in the closed-shell representation). The first excited state, which is dominated by the closed-shell configuration (two electrons in HOMO), is found at about 1700 cm^{-1} above the lowest singlet state. We suggest that the bleaching effect is due to the TICT excited state formation. After excitation the molecule will start to twist. During the twist the character of the excited state starts to change. The twisted excited state will

decay to a twisted local minimum on the ground state potential energy surface. Since the triplet state is very close in energy there is also a good chance to populate the triplet state. The absorption spectrum for the irradiated solution should hence be calculated using the geometry obtained for the twisted excited state. The initial state of the absorption process is the open-shell biradical state obtained by a restricted open-shell Hartree-Fock calculation followed by a CIS calculation in which all single excitations, corresponding to $\pi \rightarrow \pi^*$ and $n \rightarrow \pi^*$ transitions from both the closed-shell and open-shell reference determinant were included. The absorption spectra of P3CNQ before and after bleaching are displayed in figure 6. The triplet-triplet spectrum obtained using the twisted geometry looks similar to the singlet-singlet spectrum presented in figure 6.

* Fig 6. *

In the observed absorption spectra of the irradiated solution the charge transfer band, that gives the color, has disappeared and the band at about 30000 cm^{-1} has gained intensity compared to the band found at that energy in the non-irradiated molecule. The charge transfer bands have completely disappeared in both predicted absorption spectra when we calculate the spectra using the twisted geometries. We predict the first band to appear at about 30000 cm^{-1} for both molecules, with a larger oscillator strength compared to the band at the same energy using the non-twisted geometries and closed-shell description. Although, the band appears at the same energy in both the non-irradiated and the irradiated solution, the character of the transition is not the same. The calculated spectra compare very well with the experimentally observed spectra. The re-coloring of the solution is due to thermal equilibration back to the global minimum, and the non-twisted ground state is slowly repopulated. Irradiated L-B film remains colorless for several years [2a].

The charge transfer band of non-irradiated L-B films is found at much higher energies compared to solvent spectra. In order to investigate the L-B film absorption spectra of P3CNQ and Q3CNQ we have performed calculations on dimer complexes of the two systems. The monomer units are aligned in a parallel fashion as suggested by the geometry of the mono-layers in the non-central-symmetric Z-type L-B film. We have performed calculations at monomer separation distances between 3.5 Å and 5.5 Å. The monomer separation distance in the solid state is about 3.5 Å [17]. The predicted absorption

spectra of L-B films P3CNQ and Q3CNQ are compared with the observed spectra in table 3. The predicted spectra in table 3 are calculated using a monomer separation distance of 5.5 Å. For comparison a gas phase calculation of P3CNQ is included in table 3. We have previously reported calculations on solid state absorption spectrum of α-P3CNQ [1c], where we found a very large dimer interaction. In the L-B film calculations we see an even larger dimer interaction. These calculations suggest that transitions at about 26,400 cm-1 in P3CNQ films might be sought.

4.3 The rectifier character of Q3CNQ.

It is experimental known that the metal/L-B film/metal junction show an asymmetric I-V characteristic if an electric field is applied over the junction [4]. If the L-B film is bleached, the asymmetry disappears and the conductivity is very small and independent of field direction [4b].

In principle we have four steps in the conduction mechanism. First the electron must be transferred from the electrode to the first layer of the L-B film. The second step is an intra-molecular electron transfer where the electron is transferred from the donor part to the acceptor part of the L-B film. The third step is an inter-molecular electron transfer where the electron is transferred from one layer to the next layer. The fourth step is an electron transfer from the last layer to the second electrode.

The first and fourth step in this mechanism can be achieved by adjusting the external potential in a way so that the Fermi level of the electrodes approaches the orbital energy of the HOMO of the L-B film. When the Fermi level of the electrodes and the HOMO energy is equal, electrons or holes can be transferred from the electrode and the molecules. Step two and three is restricted by molecular factors, the geometry of the polar group and the relative geometry of the mono-layers in the L-B film. Thus, we focus on step two and three in the above mechanism. To achieve good conductivity the activation barrier for the electron must be small and the electronic coupling between the donor and acceptor must be large. As was discussed in the theory part we search for a situation where donor-acceptor character of the polar group disappears. When that happened, electrons are delocalized over a large part of the molecule. The experience from the geometry optimizations showed that the zwitterionic conformation was stabilized in a reaction field. The effect of the reaction field is the same as the reversed bias would

have on the geometry. On the other hand in the forward bias situation the electric filed would favor the delocalized conformation. The most favorable situation for the conductivity is obtained when the geometry of the polar group is completely planar. The HOMO is then delocalized over the whole π system, but there is still no amplitude on the hydrophobic tail. Thus, the second effect of the electric field in the forward bias mode is to create a more favorable situation for the electron transport through each layer in the L-B film. Assuming Koopmans' approximation that equates occupied orbital energy with ionization potentials [18], Δ may be obtained as the orbital energy difference between the HOMO and HOMO-1 for the N+1 electron system at the avoided crossing of the two potential energy surfaces [19]. N is the number of electrons in the actual electron transfer system. The calculated internal reorganization energy due to the twist is calculated to be 0.08 eV and the corresponding electronic coupling is calculated to be 1.39 eV. Thus, the intra-molecular electron transfer is clearly adiabatic. However, the crucial step is the inter-molecular electron transfer step since the molecular orbitals are still localized on the π systems of the molecules in one layer. The interaction between the π systems inside each layer are large but even in high electric filed the interaction between the layers is small. If no penetration between the layers occurs the closest distance between two polar head groups is about 25 Å or even larger. We have calculated the electronic coupling between two layers and get an upper limit of 10^{-8} eV for Δ. Since geometry changes will affect the calculated Δ value we prefer to just present an approximate upper value. From the above estimate of Δ it is clear that to obtain adiabatic electron transfer large changes or penetration between the layers must occur. From this discussion we conclude that the asymmetry of the measured I-V curve might have a molecular origin, but the electron transport through the film is highly non-adiabatic. The conduction might be facilitated by defects of the L-B film. When the bias is reversed the localized character of the polar group is increased resulting in an even smaller interaction between the mono-layers in the film. It is also necessary to apply a larger filed since the molecular orbitals that are localized on the tail are found at lower energies compared to that of the HOMO.

One obvious way to increase the electronic coupling between the mono-layers would be to use a shorter hydrophobic tail but there are then problems to fabricate the L-B film. An alternative would be to use a slightly polar end group such as an ethylene group or a $COOCH_3$ group. Whether it is possible to fabricate L-B films of such materials is not clear to us but we believe that Z type L-B film will be

stabilized by such an end group [20]. By using a slightly polar end group the electronic coupling between the mono layers would increase. Hence, the critical electric field needed to achieve conduction through the film would be smaller.

5. Summary.

We have obtained geometries for the two D-b-A molecules P3CNQ and Q3CNQ. The ground state of both molecules can be described as a resonance mixture between neutral and zwitterionic form. The geometries of the first excited state for both molecules were also calculated. The donor group twist upon excitation and the excited state is of the twisted intramolecular charge transfer (TICT) state type. The twisted geometries have biradical character, and their energy minima correspond to a local minimum on the ground state potential energy surface. The TICT state formation explains the bleaching that occurs in solutions of both molecules as well as the bleaching of the L-B films of the molecules. As was also found for the solid state absorption spectrum of α-P3CNQ [1c] the dimer interaction is calculated to be very large for both Q3CNQ and P3CNQ. The dimer interaction is the major contribution to the large red shift of the charge transfer band when comparing the absorption spectrum of L-B film and acetonitrile solution of both Q3CNQ and P3CNQ.

The observed asymmetry of the I-V curve obtained when an electric field was applied over a metal/L-B film/metal junction of Q3CNQ is explained using a local intramolecular electron transfer model. The D-b-A molecule is characterized by a potential energy surface with two minimums; one representing the closed-shell, delocalized ground state, the other a charge separated state. Under forward biasing the high energy charge separated state is lowered in energy. The electronic coupling is very large and the intramolecular electron transfer is adiabatic. However, the rate determine step is the inter-molecular electron transfer between the layers of the L-B film and that step is predicted to be highly non-adiabatic. Thus, the electron transport must take place trough defects of the L-B film.

We suggest a way to increase the conductivity through the film by changing the end group of the hydrophobic tail.

6. Acknowledgments.

This work was supported in part by grants from the Office of Naval Research and the National Science Foundation (CHE9312651). A. Broo is grateful for support from the Swedish Natural Science Research Council (NFR).

7. References

1. a) A. Broo, Chem. Phys. **169**, (1993), 135;
   b) A. Broo, Chem. Phys. **169**, (1993), 151;
   c) A. Broo and M.C. Zerner, previous paper in this journal.
2. a) G.J. Ashwell, Thin Solid Films, **186**, (1990), 155;
   b) G.J. Ashwell, E.J.C. Dawnay and A.P. Kuczynski, J. Chem. Soc. Chem. Commu. **19**, (1990), 1355.
3. A. Broo, in Computations for the Nano-Scale, eds. P.E. Blöchl, C. Joachim and A.J. Fisher, NATO ASI series **E240**, Kluwer Academic Publisher, Amsterdam (1993), 163.
4. a)G.J. Ashwell, J.R. Sambles, A.S. Martin, W.G. Parker and M. Szablewski, J. Chem. Soc. Chem. Commun, **19**, (1990), 1374;
   b) A.S. Martin, J.R. Sambles and G.J. Ashwell, Phys. Rev. Letters **70**, (1993), 218.
5. R.M. Metzger and C.A. Panetta New J. Chem. **15**, (1991), 209.
6. D. Bloor, Phys. Scr. **T39**, (1991), 380.
7. A Aviram and M.A. Ratner, Chem. Phys. Letters **29**, (1974), 277.
8. see e.g. R.A. Marcus, J. Chem. Phys. **43**, (1965), 679;
   N.S. Hush, Trans. Far. Soc. **57**, (1961), 557
9. a) MOPAC 6.0 Program 455, Quantum Chemistry Exchange.
   b) PM3, J.J.P. Stewart, J. Comp. Chem. **10**, (1989), 209.
10. GAMESS, M.W. Schmidt, K.K. Baldridge, J.A. Boatz, T.S. Elbert, M.S. Gordon, J.H. Jensen, S. Koseki, N. Matsunaga, K.A. Nguyen, S. Su, T.L. Windus, M. Dupuis, J.A. Montgomery Jr. J. Comp. Chem. **14**, (1993), 1347.

11. ZINDO M.C. Zerner, Quantum Theory Project, University of Florida, Gainesville, Florida 32 611; see also J.E. Ridley and M.C. Zerner, Theoret Chim. Acta **32**, (1973), 111.

12. M.M. Karelson and M.C. Zerner, Int. J. Quant. Chem. Symp. **20**, (1986), 521;
M.M. Karelson and M.C. Zerner, J. Phys. Chem. **96**, (1992), 8991.

13. N.R. Kestner and J. Logan, J. Phys. Chem. **78**, (1974), 2148;
J. Ulstrup and J. Jortner, J. Chem. Phys. **63**, (1975), 4358;
J. Jortner, J. Chem. Phys. **64**, (1976), 4860;
B.S. Brunschwig, J. Logan, M.D. Newton and N. Sutin, J. Am. Chem. Soc. **102**, (1980), 5798;
A.M. Kuznetsov and J. Ulstrup, J. Chem. Phys. **75**, (1981), 2047.

14. K.V. Mikkelsen and M.A. Ratner, Chem. Rev. **87**, (1987), 113.

15. a) A. Broo and S. Larsson, Chem. Phys. 161, (1992), 363 and references therein;
b) M.B. Robin and P. Day, Advan. Inorg. Chem. Radiochem. **10**, (1967), 247.

16. a) E. Lippert, W. Luder, F. Moll W. Nagele, H. Boos, H. Prigge, I. Seibold-Blankenstein, Angew. Chem.**73**, (1961), 695;
b) W. Rettig, Angew. Chem. Int. Ed. Engl. **25**, (1986), 971 and references therein;
c) D. Braun and W. Rettig, Chem. Phys. **180**, (1994), 231 and references therein.

17. R.M. Metzger, N.E. Heimer, G.J. Ashwell, Mol. Cryst. Liq. Cryst. **107**, (1984), 133;
S. Akhtar, J. Tanaka, R.M. Metzger and G.J. Ashwell, Mol. Cryst. Liq. Cryst, **139**, (1986), 353.

18. T.A. Koopmans, Physica **1**, (1933), 104.

19. A. Broo and S. Larsson, Chem. Phys. **148**, (1990), 103;
M. Braga, A. Broo and S. Larsson, Chem. Phys. **156**, (1991), 1.

20. A. Ulman in "An introduction to ultrathin organic films from Langmuir-Blodgett to Self-Assembly." Academic Press Inc. (1991), pp 124.

Figure and Table captions.

Figure 1.

The chemical structure and the possible resonance structure of a) P3CNQ and b) Q3CNQ.

Figure 2.

A schematic double well potential energy surface. The reaction coordinate (x-axis) is to be understood as the vibrational normal mode that takes the molecule-solvent complex from the reactant configuration to the product configuration.

Figure 3.

a) The double well potential energy surface that corresponds to a negative bias. b) The double well potential energy surface that corresponds to the case where no electric field is applied. c) The double well potential energy surface collapses into a single well corresponding to a forward bias.

Figure 4.

The predicted geometry of P3CNQ. a) The geometry of the ground state obtained using the 4x4CI/PM3 approach. b) The geometry of the first excited state obtained using the 4x4CI/PM3 approach.

Figure 5.

The predicted geometry of Q3CNQ. a) The geometry of the ground state obtained using the 4x4CI/PM3 approach. b) The geometry of the first excited state obtained using the 4x4CI/PM3 approach.

Figure 6.

The predicted absorption spectrum, in acetonitrile solution, of a) P3CNQ and b) Q3CNQ before and after beaching. Full lines correspond to "before bleaching" absorption spectra and dashed lines correspond to "after bleaching" absorption spectra. The band shape has been obtained by

superimposing Lorentzian functions centered on each calculated transition. The band width of each Lorentzian function was taken from the observed band of the first strong peak, and the area is set equal to the calculated oscillator strength.

Table 1

The composition of the ground state and first excited state for P3CNQ at the predicted ground state geometry and the predicted first excited geometry. The composition is obtained from the eigenvectors from the 4x4CI calculation. H = highest occupied molecular orbital in the closed-shell reference determinant, L = lowest unoccupied molecular orbital in the closed-shell reference determinant.

	Ground state of P3CNQ "planar" geometry	Excited state of P3CNQ "planar" geometry	Ground state of P3CNQ twisted geometry	Exited state of P3CNQ twisted geometry
H(↑,↓)	64	32	-	100
H(↑),L(↓) + H(↓),L↑)	23	62	100	-
L(↑,↓)	13	5	-	-

Table 2

A comparison between the calculated and the observed absorption spectra of P3CNQ and Q3CNQ. The observed spectra are those from reference 2a.

P3CNQ					Q3CNQ			
Calculated, μ_{gs}=31.0 D			Experimental		Calculated, μ_{gs}=29.6 D			Experimental
E(kK)	$f$osc	μ(D)	E(kK)	ε_{mol}	E(kK)	$f$osc	μ(D)	E(kK)
15.8	2.07	21.1	15.5	3900	15.3	2.03	21.2	14.0
29.8	0.06	29.7	30.3	1500	29.1	0.10	24.1	26.5
30.8	0.09	22.3			32.7	0.13	23.0	28.7

Table 3

A caparison between the calculated and the observed absorption spectra of L-B films of P3CNQ and Q3CNQ. The observed spectra are those from reference 2a.

P3CNQ monomer, calculated		P3CNQ film, calculated		P3CNQ, observed	Q3CNQ film, calculated		Q3CNQ, observed
E(kK)	$f$osc	E(kK)	$f$osc	E(kK)	E(kK)	$f$osc	E(kK)
16.6	2.59	14.4	0.0		13.9	0.0	
		19.5	6.09	20.2 s	18.8	5.69	17.7 s
30.0	0.05	26.3	0.01		25.6	0.03	
		26.4	0.12		25.7	0.03	
31.1	0.10	30.0	0.0	32.0 b	28.5	0.0	25.7 b
		30.0	0.07		29.6	0.35	
		32.2	0.01		30.1	0.04	
		32.3	0.14		31.2	0.0	
					31.3	0.03	28.1 sh
					31.5	0.0	
					31.9	0.0	
					32.5	0.06	
					33.3	0.07	

s= sharp peak

b= broad band

sh= shoulder

P3CNQ

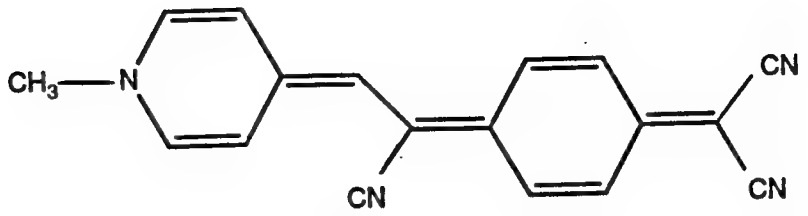

Neutral

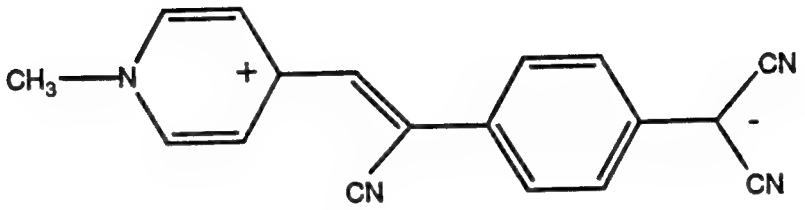

Zwitterion 1

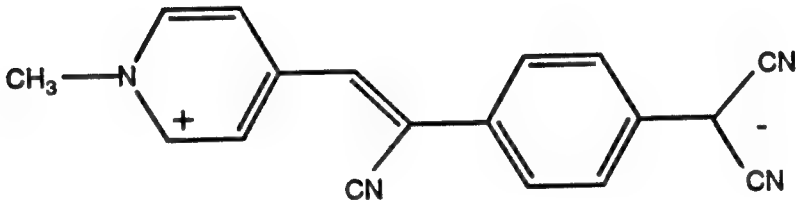

Zwitterion 2

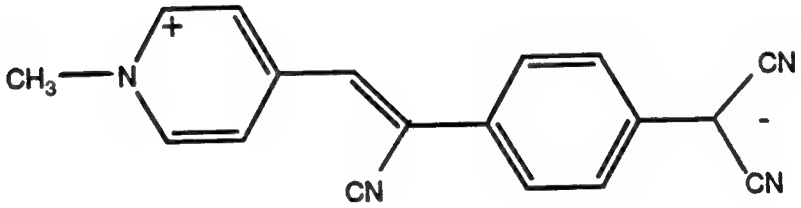

Zwitterion 3

Q3CNQ

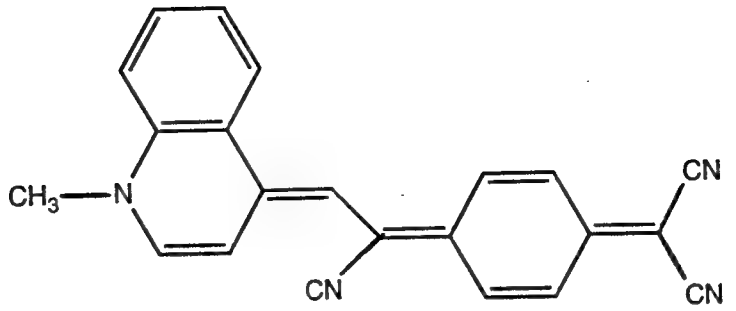

Neutral

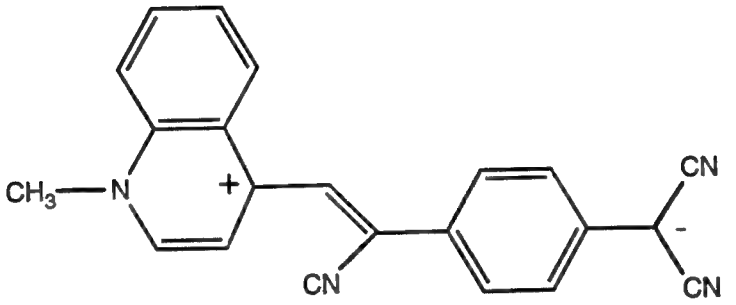

Zwitterion 1

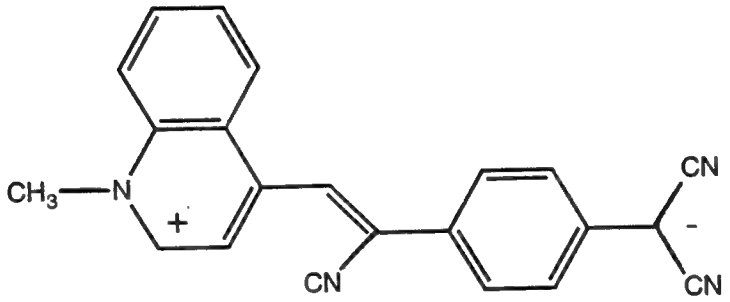

Zwitterion 2

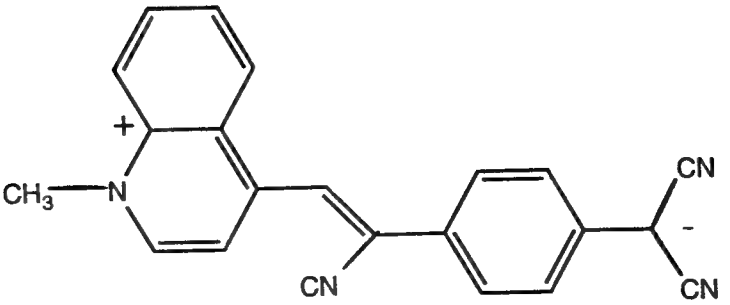

Zwitterion 3

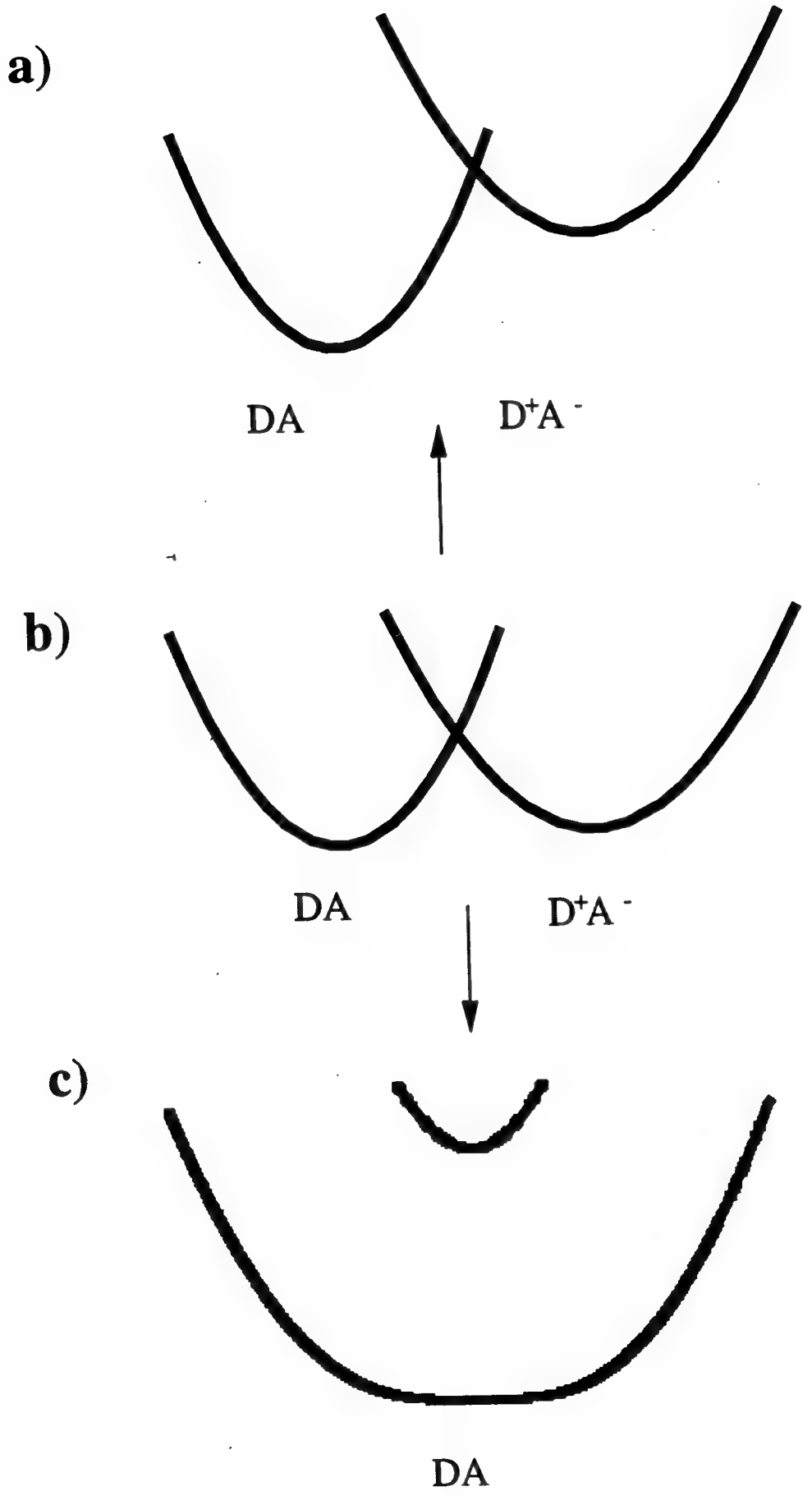
a)
DA
D+A -
b)
DA
D+A -
c)
DA

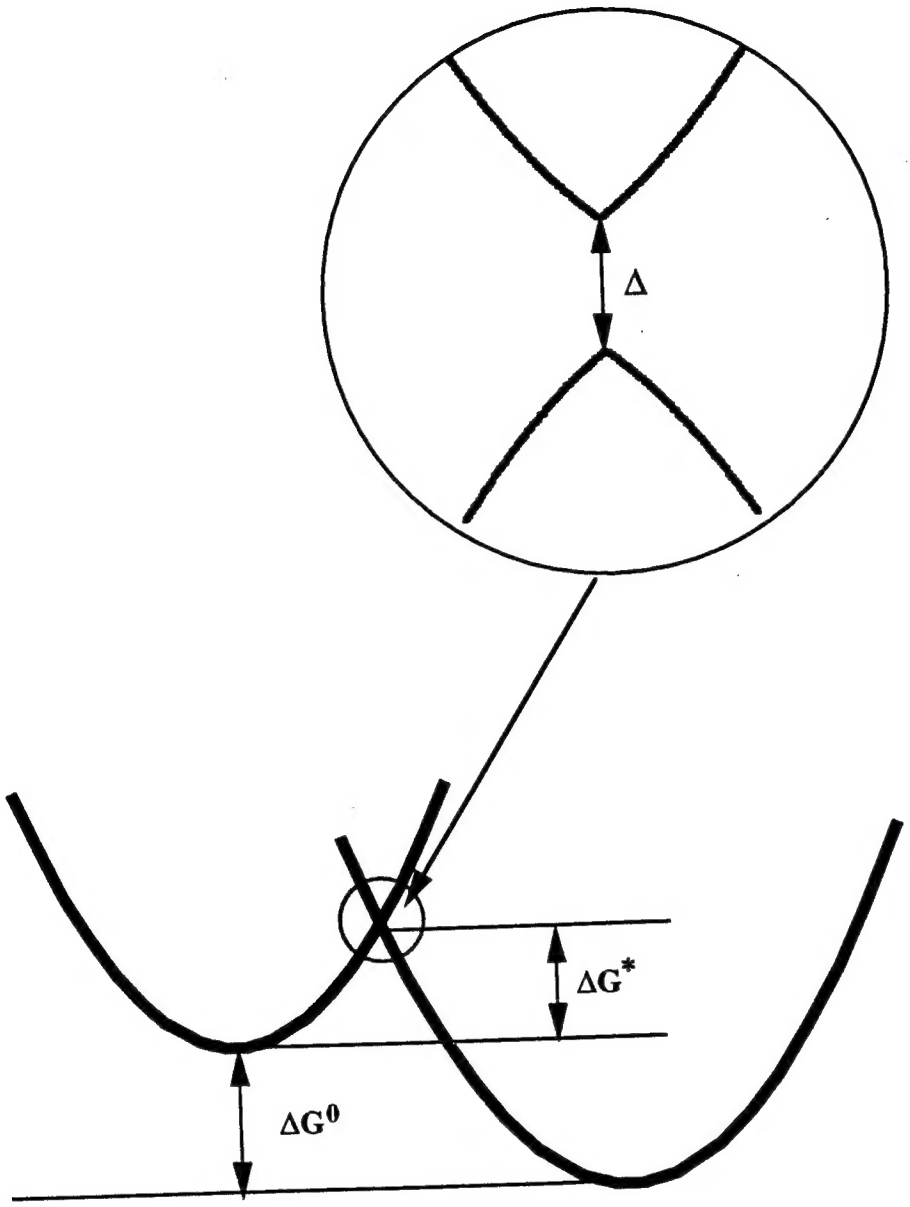
Δ
ΔG*
ΔG⁰

P3CNQ ground state

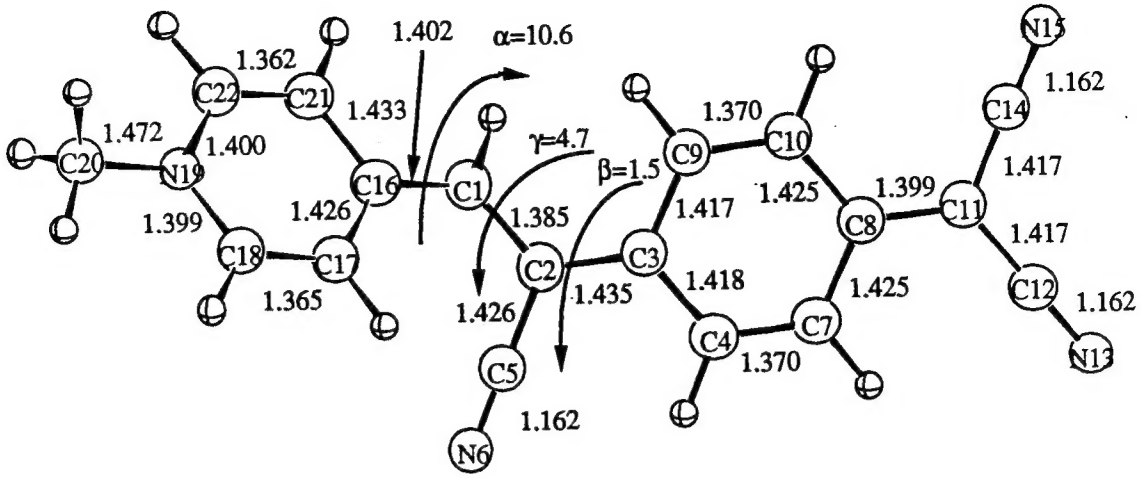

P3CNQ excited state

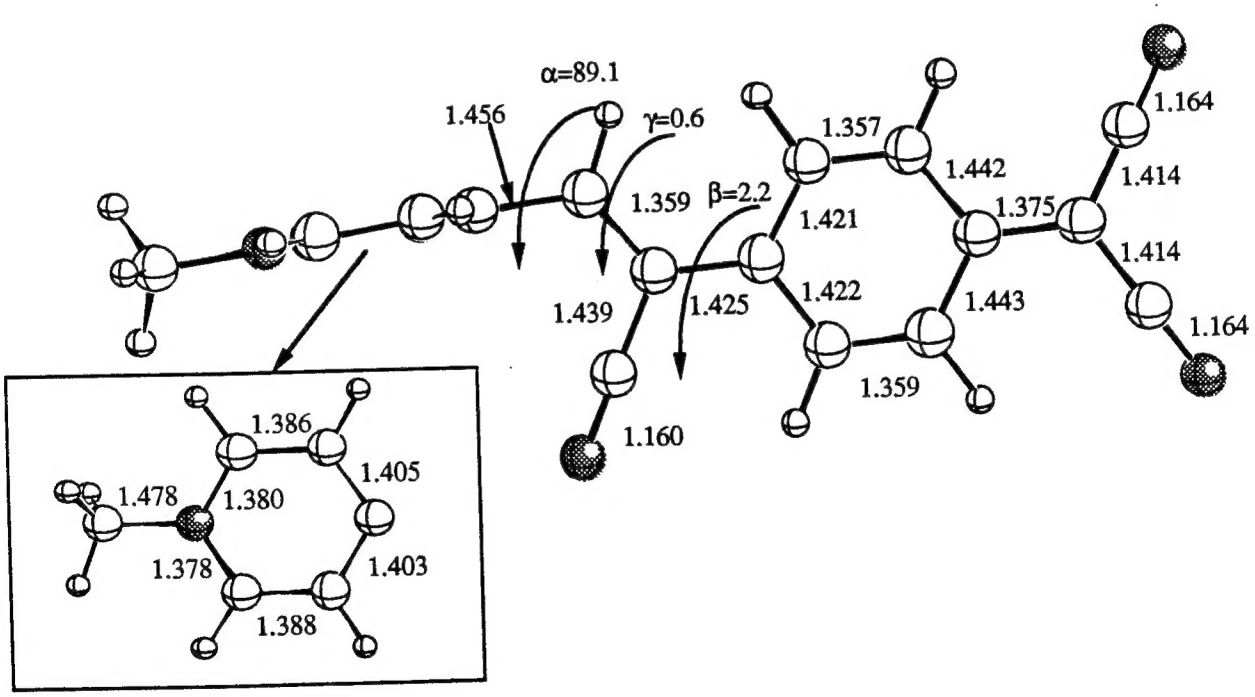

Q3CNQ ground state

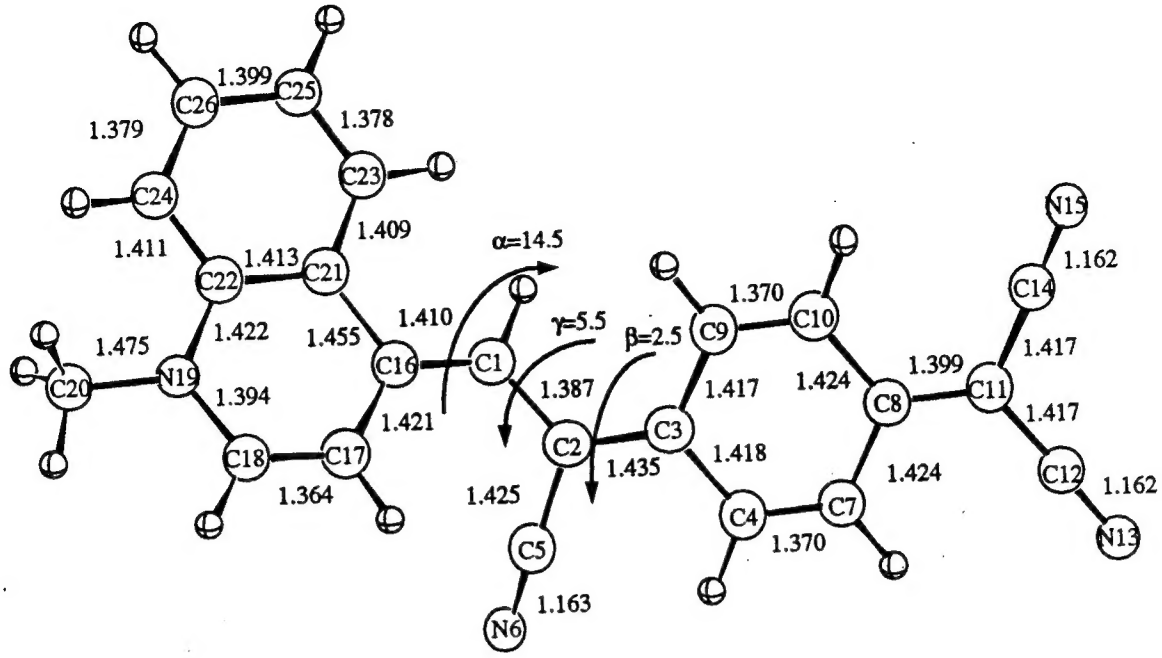

Q3CNQ excited state

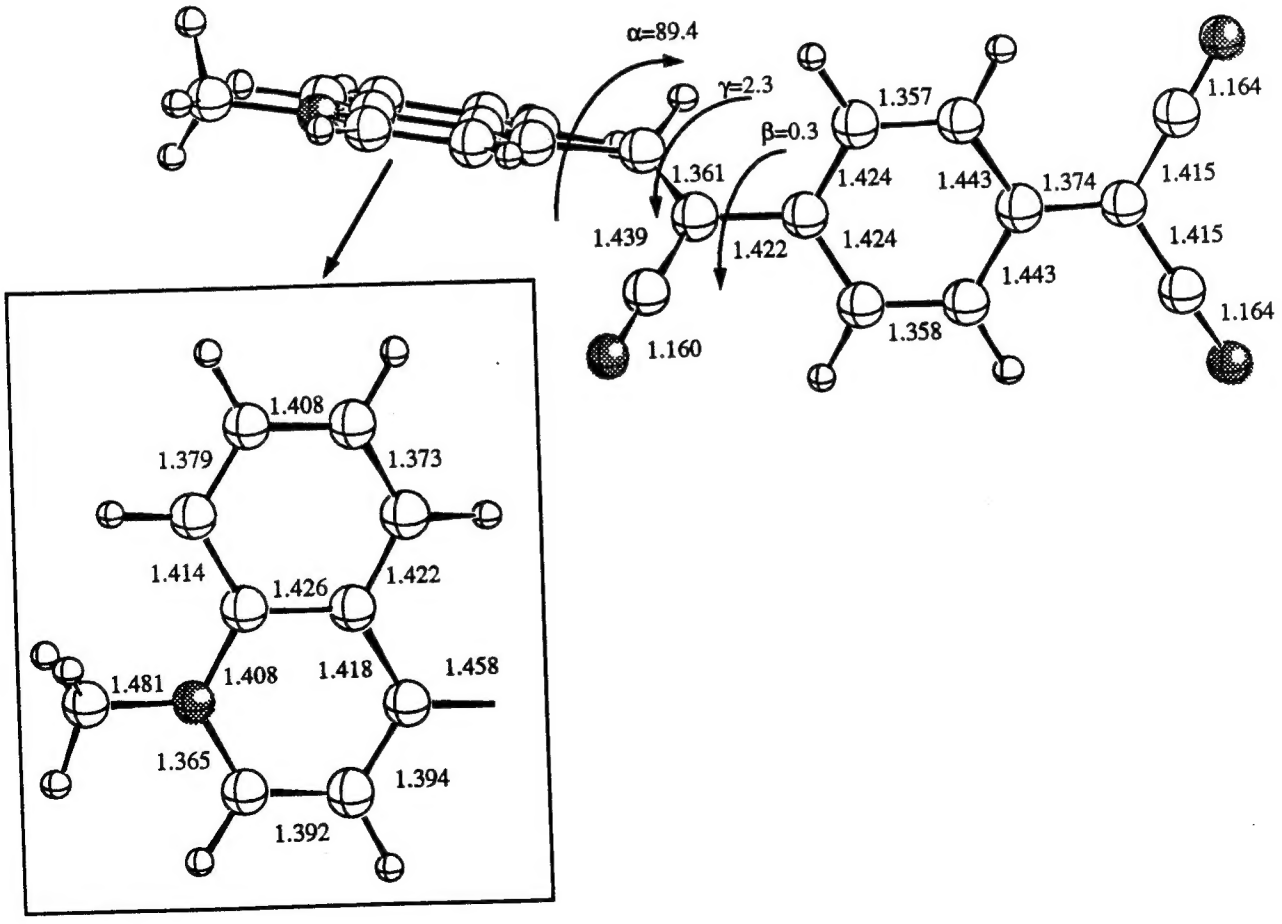

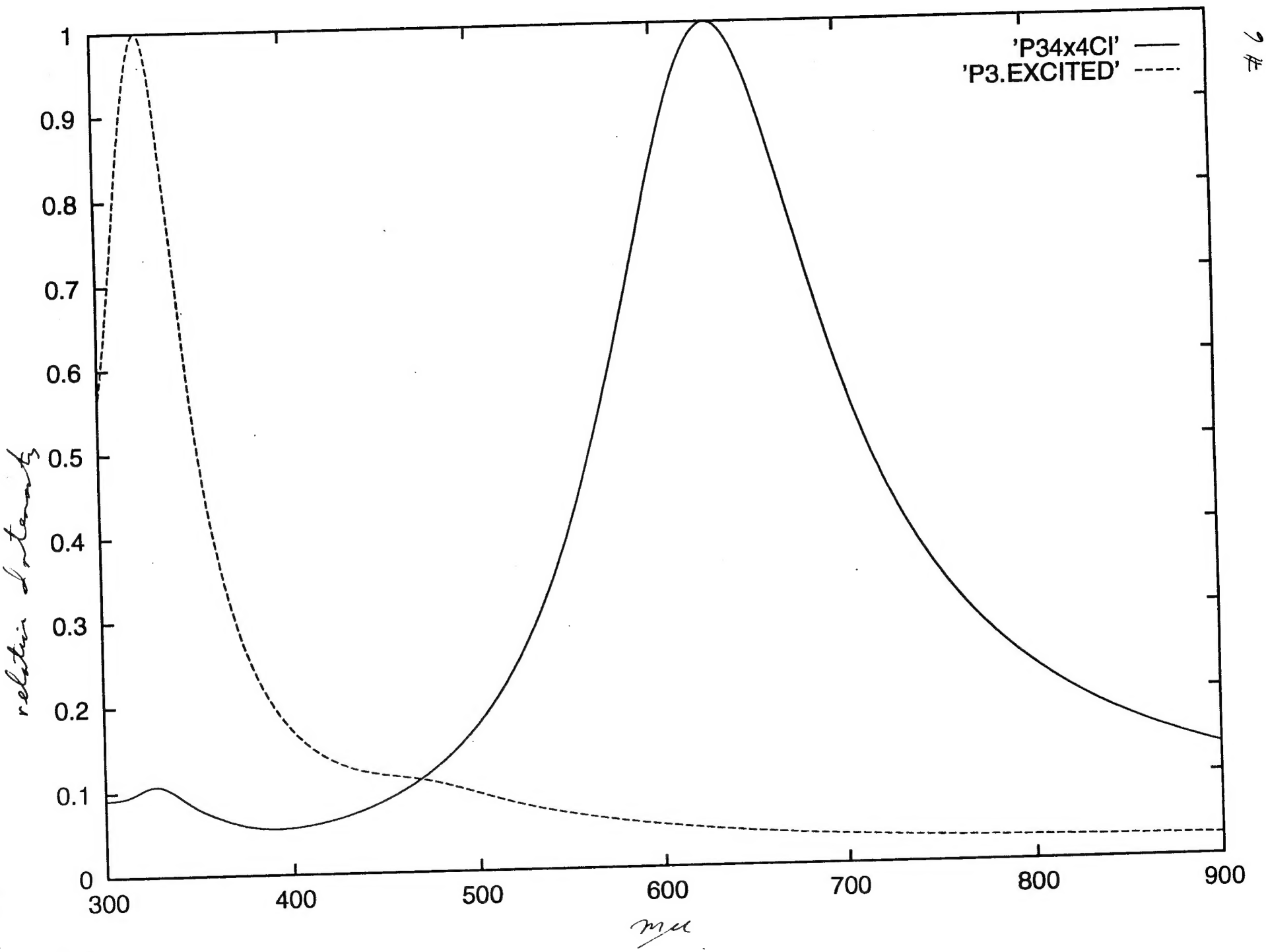
'P34x4Cl'
'P3.EXCITED'
1
0.9
0.8
0.7
0.6
0.5
0.4
0.3
0.2
0.1
0
300
400
500
600
700
800
900
relative intensity
nm